Shuttle Radar Topography Mission (SRTM) Flight System Design and Operations Overview

Yuhsyen Shen*, Scott J. Shaffer, and Rolando L. Jordan

Jet Propulsion Laboratory
California Institute of Technology
4800 Oak Grove Drive, Pasadena, CA 91109

ABSTRACT

This paper provides an overview of the Shuttle Radar Topography Mission (SRTM), with emphasis on flight system implementation and mission operations from systems engineering perspective. Successfully flown in February, 2000, the SRTM's primary payload consists of several subsystems to form the first spaceborne dual-frequency (C-band and X-band) fixed baseline interferometric synthetic aperture radar (InSAR) system, with the mission objective to acquire data sets over 80% of Earth's landmass for height reconstruction. The paper provides system architecture, unique design features, engineering budgets, design verification, in-flight checkout and data acquisition of the SRTM payload, in particular for the C-band system. Mission operation and post-mission data processing activities are also presented.

The complexity of the SRTM as a system, the ambitious mission objective, the demanding requirements and the high inter-dependency between multi-disciplined subsystems posed many challenges. The engineering experience and the insight thus gained have important implications for future spaceborne interferometric SAR mission design and implementation.

Keywords: Shuttle Radar Topography Mission (SRTM), interferometric synthetic aperture radar (InSAR), synthetic aperture radar (SAR), InSAR system engineering, InSAR system Performance

1. INTRODUCTION

Launched on February 11, 2000, and landed 11 days later, the Shuttle Radar Topography Mission (SRTM) successfully ended its flight after acquiring data for the generation of a near-global digital elevation model. Onboard the Space Shuttle Endeavour as the primary payload was the first spaceborne fixed baseline interferometric synthetic aperture radar (InSAR) system. The system was modified from hardware that was flown on the shuttle twice before in 1994 and operated nearly flawlessly.

The overall SRTM objective is to generate a digital elevation model (DEM) of 80% of Earth's landmass that lies within ±57° latitudes. The DEM is specified as 30m x 30m spatial posting with better than 16m absolute vertical (linear) accuracy and better than 20m absolute horizontal (circular) accuracy, all measured at 90% (1.6σ). The DEM meeting these specifications exists only sparsely globally. The SRTM derived DEM will thus increase the availability of the global DEM data with unprecedented uniformity and improved specifications. The mission was jointly sponsored by the National Aeronautics and Space Administration (NASA) and the National Imagery and Mapping Agency (NIMA). The German and Italian Space Agencies (DLR and ASI) also contributed by supplying the X-SAR system.

The use of synthetic aperture radar (SAR) as a remote sensing tool has become extensive since the SAR technique was first conceived in 1951. With its all weather and day/night operation capabilities, together with unique target signatures in the microwave regime and high-resolution wide-coverage imagery, SAR has found a great variety of applications as powerful science research and military surveillance instruments. It has been implemented on both airborne and spaceborne platforms. Over time, capabilities such as multiple frequency and multiple polarization have been explored and implemented, with the latter leading to SAR polarimetry. SAR systems have also became more versatile in operation capabilities. Using phased

* Correspondence: E-mail: yuhsyen.shen@jpl.nasa.gov; Voice: 818-354-7075; Fax: 818-393-6943

array antennas, operational modes such as scanning SAR, to increase swath coverage, and spotlight SAR, to improve resolution, were developed. The evolution of the SRTM system began with a series of SAR missions sponsored by NASA over the past two decades. Starting from SEASAT (1978), which was the first demonstration of spaceborne SAR, to SIR-A (1981), SIR-B (1984) and SIR-C (1994). Of these missions, SIR-C[1] (Spaceborne Imaging Radar-C) represents the single largest enhancement in capabilities from its predecessors. SIR-C was a dual frequency (in L- and C-band) and full polarimetric SAR system. Its operation modes included the conventional strip-mapping mode and the more advanced scanning mode and spotlight mode. With its versatile capabilities, SIR-C encapsulated SAR capabilities evolved over the last two decades. These capabilities, in particular scanning SAR and multiple polarization, had contributed to the appeal of modifying SIR-C hardware to meet the new requirements of SRTM.

In parallel to the exploitation of frequency and polarization diversities and enhanced operational capabilities, efforts in combining interferometry with SAR have also been made steadily over time, with heightened interest and intensified research in recent years[2]. The primary InSAR applications are for generating topographic data, or height reconstruction, and for surface change detection and monitoring, depending on system configuration and operation. InSAR requires a pair of images. For topography derivation, the image pair would be preferably acquired at the same time but from slightly different perspectives separated by a baseline. This is known as a single pass InSAR. If the two antennas producing the image pairs are connected by a rigid structure, it is call fixed baseline InSAR. For change detection, the image pair would be preferably acquired at different times, but with the exact same perspective. This is known as the repeat-track InSAR. A variation of the above two preferred and ideal configurations is to use the repeat-track InSAR configuration for height reconstruction. This requires the changes, either from the surface features or characteristics of atmosphere, between the two repeat visits, be negligible and the tracks can be controlled to form an acceptable baseline. The reconstructed height accuracy may be seriously compromised, if it can be reconstructed at all, if significant changes occurred between visits. A proof of concept of using this technique for topography derivation was demonstrated by using SEASAT data. Similar experiments were subsequently performed with data acquired from SIR-C flights and other SAR satellites, such as ERS-1/ERS-2 and JERS-1.

For height reconstruction, the fixed baseline InSAR has the unique advantage over the repeat-track InSAR because (a) the image pair is acquired simultaneously, minimizing the errors introduced by changes, and (b) the baseline is better controlled and nearly constant, reducing the complexity of height reconstruction. Although the fixed baseline InSAR has been implemented for several airborne platforms, the implementation of a spaceborne InSAR poses significant challenges for the need of a dual channel radar system whose two antennas have to be separated by a precisely measured and well-maintained baseline. Before or at the same time when SRTM was being proposed, several InSAR concepts were studied for global topography generation, including free-flying twin-satellite InSAR systems and free flying fixed baseline InSAR systems over different frequencies. Modifying SIR-C hardware to form a fixed baseline InSAR, later named SRTM, turned out to be the most cost-effective and quickest approach to obtain the near-global DEM.

The remainder of this paper focuses on the C-band InSAR system implementation. The L-band capability of the SIR-C design was not needed and not available for SRTM. The German/Italian-contributed X-band InSAR system, while an integral part of the mission, was mainly in radar electronics, not a complete representative for an InSAR implementation. Furthermore all the X-SAR functions and activities can find their counterparts in the C-band InSAR implementation. It must be noted that, however, for the given SRTM baseline length of 61 m, being operating at X-band (9.1 GHz) and operating as in strip-mode (as opposed to C-band's scanning SAR mode), the X-band InSAR can achieve better height accuracy in the regions that they collect data, but cannot achieve near global coverage. As is the case for all SAR systems, the shuttle performance can influence the quality of data products and the complexity of data processing. We will discuss the shuttle performance in the context of how it affects data acquisition and quality, not its overall mission operations.

2. SYSTEM ARCHITECTURE AND SPECIAL DESIGN CONSIDERATIONS

The C-band InSAR can be divided into flight and ground segments, each consists of several systems. This section briefly describes the functions of each system and unique design features for SRTM.

2.1. Flight Segment

There were three systems to form the payload, excluding the X-SAR, the shuttle and the shuttle interface hardware. Redundancy was included in design whenever it was required, for safety reasons, or it was practical and resources were available; however, there were still a few single-point failures in the design that could lead to loss of science data. Figure 1 shows the flight segment of the payload when the mast is deployed, with key components indicated.

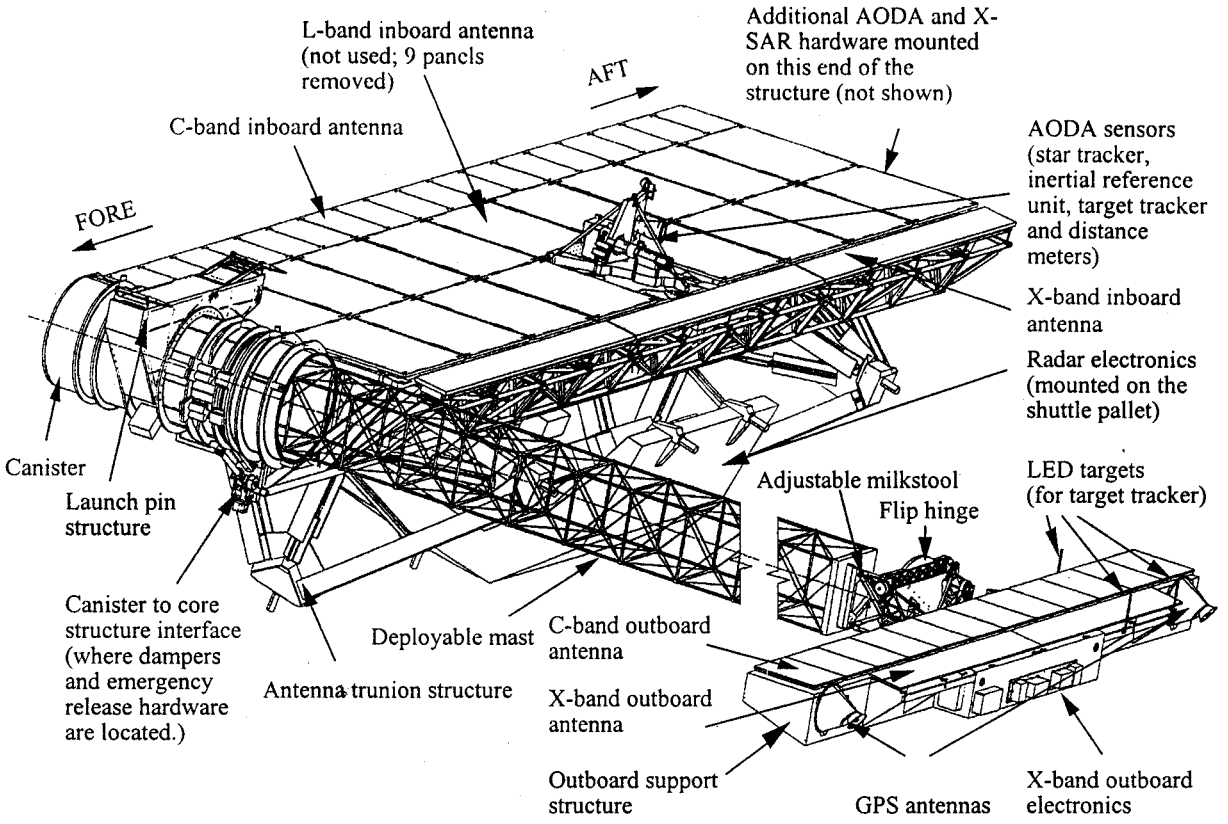

Figure 1: SRTM payload deployed configuration.

(1) C-Radar System (C-RADAR)

The C-RADAR was built upon previously flown SIR-C radar hardware by adding a new antenna and other modifications. As an interferometer, C-RADAR generated and transmitted pulses from the original C-band antenna, located inside the cargo bay (referred to as the inboard antenna). The returned signals were received from both the inboard antenna and a newly built outboard antenna mounted on the outboard structure. The new receive-only antenna used a similar design, but newer technology, to ensure both antennas can be controlled and performed similarly. Both antennas were distributed active phased array with dual polarization (H and V). The dual-pol active phased array antennas were key to achieving the swath width necessary to support a 10 day global mapping mission. During data acquisition, the inboard antenna formed the H-polarization and V-polarization beams simultaneously to illuminate the target area but pointed at two different sub-swaths. As such, two sub-swaths of the entire swath (of 225 km) were illuminated at any time. Upon receive, both antennas formed dual polarization beams in a direction slaved to the inboard antenna beams to capture the returned signals. These simultaneous two beams were steered electronically to illuminate another two sub-swaths, completing the four sub-swath coverage, in a ScanSAR operation. Four receive channels were required to capture the signal: one for each of the two polarization beams and one for each inboard and outboard antenna, which were made available by modifying the existing SIR-C two L-band channels. This simultaneous dual-polarization ScanSAR operation was required to increase the sensitivity of the radar, thus better height accuracy. C-RADAR also had a contingency mode of operating with a single polarization with four sub-swaths ScanSAR, with slightly reduced sensitivity.

Residual errors, which could not be compensated, phase between the two interferometric channels in particular, translate to uncertainty in height. Calibration tone (caltone) signals were injected to the receiver channels to track system variation, and during post-mission processing, to compensate for the variation. To maintain the stability of the caltone signals for the outboard channels, the caltone was routed through a self-compensating optical link.

To mitigate potential inboard/outboard antenna misalignment, which if too large could reduce the radar sensitivity, the outboard antenna was deliberately made shorter than the inboard antenna. In addition, an automatic beam tracker was implemented for the outboard antenna. When activated, the outboard antenna would form additional beams to allow detection

of inboard and outboard antenna misalignment and compensate for the misalignment, by steering the outboard beams to follow the inboard transmit beams. This was the only effective means to counter rapid misalignment variations during the data take. (During the mission, this automatic beam tracker was activated for a short period but was deactivated as the inboard and outboard antennas were adequately aligned that using the tracker would not improve performance but may complicated processing.)

During data acquisition, C-RADAR was recording radar data at 180Mbits/sec using refurbished SIR-C high rate data recorders. At this rate, a data storage cassette could only stored up to 30 minutes worth of data. A few data takes would be longer than 30 minutes. Additional hardware, implemented on a laptop, was built to ensure no data were missed recorded by starting another recorder when the cassette in the active recorder was about full. This recorder control hardware also had the capability to detect faults in the recorders and performed automatic switching should that happened.

(2) Attitude and Orbit Determination Avionics (AODA)

The AODA was a brand new system designed specifically for SRTM, without SIR-C heritage. It consisted of a suite of sensors to acquire data for precision orbit (both attitude and position) and baseline vector determination.

For orbit determination, the AODA sensor suite employed a star tracker (for determining absolute attitude), an inertial reference unit (for interpolating the attitude between measurements acquired by the star tracker) and two GPS receivers (for determining the absolute positions). The star tracker and the inertial unit were mounted on the inboard antenna structure, replacing the center L-band panel, which was not needed for the mission. The GPS receivers were located on the outboard structure.

For baseline determination, the AODA sensor suite included an optical target tracker, modified from a star tracker, located on the inboard location and looking out to three LED targets mounted on the outboard structure. The data from the target tracker would be processed into baseline distance and angle. Given the locations of the target tracker and the LED targets, the distance along the mast axis would not be as precisely determined. Electronic distance meters were added to the sensor suite to acquire distance measurements along the mast axis.

All the AODA sensor data was collated and forwarded to an on-board laptop computer and the orbiter avionics via a customized interface box. The data was archived by the laptop computer and downlinked to the ground during the mission in real-time. During the mission, the crew also used the laptop to activate and control individual AODA sensors and to monitor the inboard and outboard structure alignment.

Note that during the mission, the data collected were raw unassimilated measurements. Post-mission processing would be required to process and combine these raw measurements into a data set that meets the required precision.

(3) Antenna Mechanical System (AMS)

The AMS was also built upon previously flown SIR-C hardware. The key additions were the deployable mast and the canister into which the mast was stowed. On the tip of the mast was the outboard structure to support the additional outboard electronics and antennas. The fully deployed 60m mast formed the required baseline separating the inboard antenna and the outboard antenna. The mast had to be strong and rigid to withstand the dynamic load exerted during the mission, in particular during the orbit adjustment maneuvers. In addition, the mast had to be thermally inert so that the alignment between the inboard and outboard antenna would not get seriously perturbed when on-orbit temperature varied.

Between the outboard structure and the tip of the mast was a two-degree of freedom adjustable structure, fondly called the milk-stool for its three-leg shape. The milk-stool can be adjusted to bring the entire outboard hardware into alignment with the inboard hardware.

Additional struts and trusses were built to attach the entire canister, mast and outboard hardware ensemble to the existing SIR-C structure. Dampers were included in the struts to prevent excessive motion of the tip hardware during data acquisition. Too large or quick a motion could cause the AODA or radar electronics to lose track or compromise the performance. Also at this location, a pyro-activated assembly was installed for separation of the canister ensemble from the shuttle should problems occur which prevent the mast from being stowed.

In data acquisition attitude, the payload mast was oriented at about 45° from nadir, pointed away from minimum gravity gradient. Analysis showed that there would not be enough propellant to complete the mission to maintain that attitude. By providing a small amount but continuous thrust at the tip of the mast, a cold gas subsystem was incorporated in the design to reduce the rate at which shuttle had to fire its thrusters to maintain the attitude, thus preserving enough propellant to complete the mission.

2.2. Ground Segment

The ground segment comprised of three systems, not including the X-SAR operations and processing, or the shuttle operations.

(1) Mission Operations System (MOS)
The C-band InSAR MOS comprised of five subsystems to support pre-mission planning activities and mission operations. (X-band InSAR had a similar mission operations system and mission operation team to support its operations. The C-InSAR team and X-InSAR teams were integrated in operations with the Johnson Space Center shuttle team.)

The payload operation started with the subsystem to perform mission planning. Receiving ephemeris information from JSC, Mission Planning Subsystem (MPS) would locate the opportunities to collected science data, select the proper radar configuration based on the predicted data collection geometry, divide the opportunities into units that the radar hardware can accommodate, and forward this information in 6 hour segments to the Command Management Subsystem for uplink to the flight system. This subsystem also monitored changes in the orbit and worked with JSC to plan orbital corrections when the drift exceeded preflight limits. In addition, the MPS keep track of consumables such as power, tapes, and propellant to insure that sufficient resources existed to complete the mission from the payload perspective.

Upon receipt of a command segment from the MPS, the Command Management Subsystem (CMS) performed validity and constraint checks, converted the commands to binary form recognizable by the radar, and queued them for uplink to the shuttle. Since the command link is shared by the C-band InSAR, the X-Band InSAR, and the AODA systems, the CMS operator was responsible for coordinating the link and insuring that commands were only sent during periods allocated for the payload. It was also CMS's responsibility to verify successful uplink of all C-band InSAR commands.

The Telemetry Management Subsystem (TMS) provided users visibility into almost every aspect of the payload system by accessing the raw shuttle Orbital Data stream, extracting the data corresponding to the 3 SRTM flight elements (not counting X-SAR), and distributing it to multiple users simultaneously. Since it accessed the shuttle OD, it also provided visibility into shuttle systems such as thrusters and cooling systems that affected the payload. Since all the telemetry was archived, playback of earlier data could be displayed alongside current data for trend analysis.

The Data Management Subsystem (DMS) provided a central archive to deposit and retrieve data necessary for mission operations. Because so many of the MOS Subsystems and Positions relied on the DMS for information, two identical machines were configured to mirror each other. If either one would become unavailable, the other would automatically take over.

The Performance Evaluation Subsystem (PES) was responsible for monitoring the performance of the C-band InSAR in flight, alert the POCC if any anomalies were detected that would impact the expected accuracy of the DEM, and propose updates to the radar configuration to optimize the data collection. The primary source of radar performance data was from the telemetry that included echo strength and antenna alignment information. In addition, hundreds of downlinks of raw radar data throughout the mission were processed at JPL and the results forwarded to PES for interpretation.

(2) Algorithm Development and Verification (ADV) and (3) Ground Data Processing System (GDPS)
The main activities of ADV and GDPS will occur after the mission to calibrate and process the 7 terabytes of raw radar echo data into a global height map. However, they did provide substantial feedback during the mission on the health of the system. Using components of the post-flight processing system, GDPS assembled and supported a downlink capture and storage system. Once the downlink is completed, portions of the data were then extracted, reformatted and sent on to the Radar Verification Subsystem (RVS), a subsystem of GDPS, which then generated several reports for the PES to interpret. In addition, reformatted data for selected sites would be forwarded to ADV for processing into an interferogram. Post-flight, ADV is responsible for providing the algorithms and prototype software to convert the raw radar data into height maps. During the mission, ADV used portions of that software to verify that the inboard and outboard radar channels were correlated.

3. PERFORMANCE AND DESIGN REQUIREMENTS

The SRTM was designed for a particular flight geometry during data acquisition. As shown in Figure 2, the shuttle would fly with tail forward and maintain at an attitude, which would point the antenna boresight at 45° from nadir. This geometry was dictated by the need to look to the north and cover the minimum 225 Km swath per orbit.

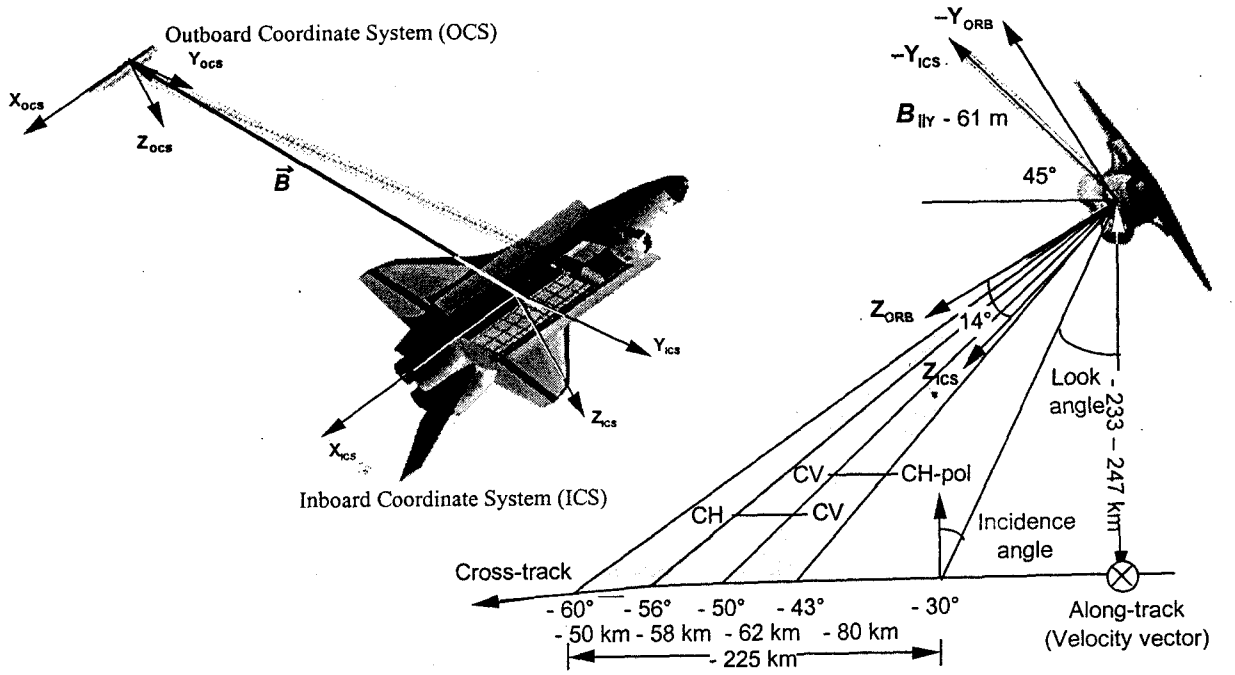

Figure 2: SRTM data acquisition geometry. Also shown is the 4-beam (4-sub-swath) coverage, to acquire the 225 km full swath, and the relevant coordinates. It also shown the polarization beam pair (CH-CV) which co-existed at the same time.

The C-band InSAR characteristics are as listed in Table 1, in particular those affecting the height performance.

Frequency	5289 MHz center carrier
Transmit signal characteristics –	Linear frequency modulated pulse with 33.8 μsec pulsewidth and 10 MHz bandwidth around carrier
Pulse repetition rate	1344 – 1700 Hz (varies)
Peak transmit RF power	1100 W
Average DC power	6250 W
Inboard TX/RX antenna (18 panels) dimension (along track x cross-track)	12.0 m x 0.75 m
Polarization	H and V independent transmit and receive polarizations
3-dB beamwidth (along track; cross-track)	0.25°; 5-14° (varies using beam spoiling)
Steerable range (along track; cross-track)	±20.0°; ±1.0°
Directivity (unsteered/unspoiled)	43 dBi
Noise temperature	800 K
Outboard TX/RX antenna (12 panels) dimension (along track x cross-track)	8.0 m x 0.75 m

Polarization	H and V polarizations
3-dB beamwidth (along track; cross-track)	0.35°; 5-14° (varies using beam spoiling)
Steerable range (along track; cross-track)	±20.0°; ±1.0°
Directivity (unsteered/unspoiled)	42 dBi
Noise temperature	500 K
Antenna boresight pointing	45°±0.5° from nadir (also baseline orientation)
Inboard receiver sensitivity	-33 dB noise equivalent sigma-0
Outboard receiver sensitivity	-33 dB noise equivalent sigma-0
Receive channels and signal polarizations	4, one each for inboard HH, outboard HH, inboard VV, outboard VV
Instantaneous data sampling rate	22.5 Msamples/sec/channel for a total of 180 Msamples
Recording data rate	180 Mbits/sec with 4 bits/sample using (8,4) BFPQ
Baseline length	61 Meters
Ground swath (look angle)	225 km (30°-58° from nadir)
Image spatial resolution (no. of looks)	30 m x 30 m (2-4 looks)
Absolute height accuracy	16 m (2 pass)
Relative height accuracy	10 m (2 pass)

Table 1: C-band InSAR parameters

System level error budgets were allocated based on those parameters that could affect the height accuracy. The allocations were the result of an iterative and trading process to make sure the total errors would meet the mission requirements but the allocations can be implemented with a particular design in mind. Table 2 shows the error budget table for the absolute height. Different error budgets were created and maintained for relative and horizontal errors as well. Note that 90% was used for the allocation of the design. These numbers were not to exceed numbers; the pre-mission predicted performance would be better, as was also shown in Table 2. The as-flown performance evaluation is still an ongoing activity as of this writing.

Parameter	Allocation (90% knowledge error)		Expected (90% knowledge error)		Contribution sources
	Parameter error	Height error	Parameter error	Height error	
1. Baseline length	3.0 mm	4.1 m	1.9 mm	2.5 m	Metrology, mechanical and phase center
2. Baseline roll angle	9.0 arcsec	15.8 m	5.2 arcsec	9.2 m	Metrology, mechanical and phase center
3. Baseline yaw angle	30 arcsec	0.2 m	20 arcsec	0.2 m	Metrology, mechanical and phase center
4. Platform position	1.0 m	1.0 m	0.9 m	0.9 m	GPS
5. Range	3.0 m	1.6 m	1.6 m	0.8 m	
6. Doppler	30 Hz	0.3 m	30 Hz	0.3 m	Can be ignored
7. Timing	100 μsec	0.7 m	100 μsec	0.7 m	Radar timing
8. Random phase	13.6°	13.0 m	13.6°	13.0 m	SNR and look dependent
9. Caltone phase	8.0°	7.6 m	6.9°	6.6 m	Residual channel random imbalance
10. Propagation	0.5 m	0.5 m	0.5 m	0.5 m	Can be ignored
11. Single pass total (RSS)		**22.3 m**		**17.5 m**	RSS of errors from 1-10
12. Reference height		1.0 m		1.0 m	
13. Calibration residual		3.2 m		2.5 m	
14. Absolute height bias		**3.4 m**		**2.7 m**	RSS of errors from 12-13
15. Cal. single pass (RSS)		**22.6 m**		**17.7 m**	RSS of errors in 11 and 14
16. Unshifted 2 pass		**15.9 m**		**12.5 m**	No mis-registration combined ($\sqrt{2}$)
17. Mis-registration		2.0 m		2.0 m	
18. Two pass total (RSS)		**16.0 m**		**12.6 m**	RSS of errors from 16-17

Table 2: Absolute height error allocation and pre-mission expectation.

Note that the height errors are particularly sensitive to three parameter uncertainties: the roll angle knowledge (item 2), the random phase (item 8), and uncompensated channel phase imbalance (item 9). The roll angle knowledge is determined by how precise the Attitude and Orbit Determination Avionics (AODA) can determine it. However, mechanical and thermal distortion of the structure, thus affecting the locations of the AODA sensors, can impact the precision of AODA results. The random phase errors vary with the number of looks attainable and system signal-to-noise ratio, both of which are in turn functions of range angle. Future free-flying InSAR systems may reduce this error contribution by having a narrower swath with more looks and building the coverage over a longer period. The caltone phase errors were the residual phase errors between the two interferometric channels. For SRTM configuration, the inboard antenna provided the illumination whereas the inboard antenna and outboard antenna served as the receiving antennas for the interferometric channel pair. Ideally, the interferometric signals, as they arrived at the antennas, contained all the information needed for height construction. However, using SRTM as an example, the inboard receive channel and the outboard receive channel were physically separated by the baseline and went through different, although similar, hardware. Any imbalance, if not compensated, between the hardware of these two channels, would introduce height errors. For SRTM, both channels were injected with a calibration tone signals, which presumably would track the changes and the effect of these changes can be removed during data processing. However, the instability of the caltone and the hardware not traversed by the caltone would lead to residual errors that could not be compensated. More complete injection path, better thermal stability, more extensive modeling may reduce this error contribution.

The error allocations for each height error influencing parameters were further converted and allocated to specifications for each component in the flight system. As an example, the allocated baseline error was further partitioned to distance meter measurement error, target tracker yaw measurement error, antenna mechanical centroid estimate error, and antenna electrical phase center error. As another example, the caltone phase error was further partitioned into antenna electrical path error, optical link compensation error, and caltone injection path error.

All the error sources listed up to Item 10 in Table 2 were specified in term of measurement precision, not accuracy. As such, the total error as listed in Item 11 reflected the errors of height against an arbitrary true and absolute height. Additional calibration using the ocean data, with a priori knowledge of ocean heights acquired from other sources, e.g. ocean altimeter, would remove the errors in absolute height. Items 12 and 13, which were totaled in Item 14, accounted for the imperfection of such absolute calibration. Since most the areas were covered twice during the mission, each pass would lead to an independent height estimate and these two can combine to further reduce height errors, with some mis-registration, as listed in Items 16 and 17.

Several aspects of InSAR implementation were of such criticality which worth brief mentioning. Definition of system and local coordinates was crucial. The entire InSAR was built piecemeal wise but each piece toward the end would be combined into a single entity and contribute to the overall performance. As an example, an error between inboard and outboard coordinate system might lead to inboard and outboard antennas to scan in opposite directions. With a set of well-defined coordinate systems and well-understood transformation between these systems, alignment measurements can then be made locally and integrated. For example, each AODA sensor location was carefully survey using a local coordinate, required for implementation expediency, but could be translated to another coordinate without ambiguity. System alignment was another critical aspect of system implementation. For AODA to be able to perform, the outboard LED targets must lie within the field of view of the inboard target tracker. Significant effort was made, through alignment measurements and simulations, to ensure once the mast was deployed the targets were indeed within the field of view of the target tracker. Lastly, a structure as large as SRTM when fully deployed the structure and mechanical aspects of it drew considerable scrutiny throughout the implementation. The structure, not only affecting the performance, which the system could achieve, it also had to meet all shuttle safety requirements.

4. MISSION OPERATIONS

The mission operations were performed primarily at the Johnson Space Center (JSC) with additional supporting activities performed at the Jet Propulsion Laboratory (JPL) and the German Space Center (DLR).

The operations at JSC followed the standard model for any shuttle mission. The shuttle operations team, residing in the Mission Control Center (MCC) and other support areas, was responsible for all operations related to the shuttle, including activities where the payload would affect the shuttle and vice versa. The payload operations team, residing in the Payload

Operations Control Center (POCC), was responsible for all operations related to the payload and providing inputs to the MCC for activities related to the shuttle operations. The main activities at the POCC included payload to MCC and crew activity coordination, payload activity coordination, data acquisition planning, payload commanding and telemetry monitoring. There was also a mission management team to coordinate and decide on key programmatic and strategic issues of the mission. The JPL team provided additional payload operations monitoring, in particular the more time-consuming trend analysis and radar high rate data processing. It must be noted that the JPL team consisted of team members who developed the flight systems or people who were intimately involved in the flight design. The use of flight system design team as the mission operation team, as opposed to have two separate teams as some missions would operate, considerably lowered the risk of mission operations and the cost.

The communications between the onboard and ground payload operations relied on (a) voice communications throughout the mission infrastructure among crew, MCC, POCC, and JPL, (b) payload command up-link from the POCC to the payload, (c) payload telemetry down-link from the payload to the POCC and to JPL, and (d) payload radar high rate data down-link from the payload to the POCC and JPL. There were also mission summary packages, payload status included, provided to the crew as the mission progressed.

The SRTM mission can be divided into three phases from the perspective of payload operations: (1) activation and on-orbit checkout phase, (2) mapping phase, and (3) deactivation phase. The actual time from launch (or the Mission Elapsed Time, MET) is used for each phase. The MET is listed as DD/HH.MM where DD is the day, starting from Day 0, HH is the hour, in 24-hour clock, and MM is the minute. Since the time is to provide an approximate reference of these phases, the seconds in the MET are not included.

4.1. Activation and On-Orbit Checkout Phase (MET 00/02:10–00/11:40)

The phase corresponds to when the crew starts to install stored payload hardware to when the payload is in the mapping configuration with all essential functions verified. The main activities were, in approximate chronological order,

- Installed and configured payload hardware in storage within the crew cabin
- Deployed and Activated the payload
- Verified command and telemetry link
- Checked proper operations of the payload as the payload was being activated and deployed
- Characterized mast structural properties
- Evaluated inboard and outboard alignment and performed necessary adjustment
- Performed payload data acquisition to assess payload performance

The integrated procedure for this period was very complicated due to inter-dependency among the steps. Also there were a few orbiter maneuvers needed to executed and orient the payload to the desired attitude and assert the desired level of attitude control. Timely execution of each step was crucial, because the entire mission duration was fixed and belatedness of completing check out phase would adversely affect the duration of the mapping phase, thus reducing the coverage. Likewise, an early completion would allow more coverage. Three on-orbit check out plans were designed and rehearsed prior to the mission, with one of them dealing with the nominal operations and the other two with contingency situations. All plans were designed to ensure the mapping phase would start on time with various levels of risk taking by eliminating or postponing some steps.

As each step was executed, there were pre-mission prescribed pass-fail criteria. Contingency measures were planned to trouble shoot or take alternate routes in case the steps were not executed successful. Obviously failure of some steps could lead to early termination of the mission.

The nominal plan, which prescribed the mapping phase to start approximately at 00/14:10 with some conservatism for unexpected anomalies, was used during the mission. The procedure was executed effectively by the well-trained team and the payload performed nearly as design upon initial activation and deployment. The payload wad declared ready to start mapping on 00/11:40, about 2.5 hours earlier than the nominal plan prescribed.

However, later analysis of the data acquired during the on-orbit checkout phase indicated that all the dampers were not functioning after being uncaged but there was no impact to the payload performance, thanks to the design margin. The dampers were subsequently caged and not used throughout the mission.

4.2. Mapping Phase (MET 00/11:40–09/18:10; for a total of 151 orbits)

The mapping phase started when all the essential functions of the payload were checked out and the payload was ready to performed routine data acquisition of the world. During this phase, the world was systematically mapped, interrupted only when flying over the ocean or when an orbit adjustment was needed.

The activities during this phase were broken into repetitive 6-hour planning and execution cycles. The cycle started with the mission planner generated a data acquisition plan for the next 6-hour cycle in advance, detailing each data take, time and duration. In order to do this, the orbiter position and attitude had to be predicted accurately. The plan also included major shuttle events such as orbit adjustment for which the planner had to coordinate with the MCC personnel to find the opportune time for execution. Accompanying the plan were the parameters associated with the radar configuration and data routing. These parameters were then converted into the specific radar commands and up-linked via the MCC to the payload. Once a data take started, the telemetry was distributed and monitored by POCC personnel who was assigned and trained for a particular portion of the payload. The telemetry, at 128 kbits/sec, was real-time and was available nearly all the time except for a brief outage every orbit. It contains all the necessary information to monitor the status and health of the payload. It also included all the metrology avionics data.

For the radar performance, there were tools to predict, based on expected data take scenario and pre-mission models, the performance of the payload for that particular data take. These predicted performance would be compared against the actual performance as evaluated from the telemetry to certify the data take. A very small portion of the radar high rate data (recorded at 180 Mbits/sec and could be downlinked at 45 Mbits/sec) was downlinked to JPL from which more detailed assessment of radar performance and radar images were processed.

The usage of consumable and constrained resources, such as energy and tape, was also closely monitored. Approximately every 12 hours, all the as-run information would be included in a mission progress report, including quality of the data takes, the coverage area, and consumable usage of the past 12 hours. Pre-mission mapping planning included strategies to deal with different levels of consumable shortage. These mapping strategies factored in the current DEM availability, criticality of specific areas, and the overlap in coverage. The 12-hour mission summary information not only provided progress of the mission but also helped in evaluating the consumable and deciding mapping strategy as appropriate for the remaining consumable.

Several orbit adjustments were performed while the payload was fully deployed, so that the payload could perform within specifications. A special procedure, called fly-cast, was devised to control excessive bending of the mast caused by outboard tip inertia when the maneuvering pulses were applied. The fly-cast maneuver used a short pulse to trigger the mast tip motion to its equilibrium flexing point, which was about half of the full deflection if the mast tip were allow to continue to move. It was then followed by firing the long pulse required for the maneuver while the mast tip maintained at the equilibrium point. Similar steps were used to terminate the maneuver. Each of the fly-cast maneuvers was executed flawlessly during the mission.

There were three payload problems during this period and the most significant one was the failure of the cold gas system. The failure rendered the cold gas assembly ineffective in providing mitigation of shuttle propellant usage. The mission team, working together with the payload, managed to find means to alleviate the impact of cold gas failure. On the payload side, the attitude control was relaxed to reduce the propellant usage. In the end, these propellant saving measures were adequate to complete a successful mission. There were a couple of transient faults in the data recording hardware, which required reconfiguration but no impact to the data. The metrology hardware had occasional dropouts, which were recoverable because of built-in redundancy.

Note that it would require 159 orbits in order to cover the landmass at least twice, as the proposal initially required and had been planned until about 3 months before the mission. At that time, it was decided to terminate the mapping phase one day earlier to protect the possibility of having the crew to go to space to stow the payload in case of contingency. That plan of acquiring about 143-orbit worth of data was baseline for the mission. However, real-time evaluation of the payload performance and risk evaluation led to collection of 151-orbit worth of data, including the 2.5 hours earlier start of mapping. With 151 mapping orbits and near flawless operations, about 99.96% of the targeted areas in the original plan was mapped at least once (leaving <0.1% of areas not mapped) and 94.59% of the areas was mapped at least twice.

4.3. Deactivation Phase (MET 09/18:10–09/22:45)

The deactivation phase started when the last data acquisition was completed. The time allowed for executing the last data take was based largely on all the activities the shuttle had to performed to be ready for return and the consumable required to perform those activities. From the payload perspective, the deactivation procedure consisted of steps to deactivate and de-stalled the crew-cabin hardware to storage.

The most crucial step was the retraction of the mast, which would have to be jettisoned with the canister if not properly retracted and stowed. At the time of retraction, the mast had been exposed to cold temperature to the extent that the first two attempts to bring the mast into stowage were not successful, even when heaters were applied in advance. After waiting for the canister and the portion of the mast already warmed up, the stowage was completed with all latched closed.

5. POST-FLIGHT OPERATIONS

The immediate operation after the mission was to retrieve and duplicate the mission data to prevent inadvertent but irrecoverably loss. All the telemetry data and the high rate data were duplicated and copies stored at different locations. Also the as-run mission planning information and operators' logs were compiled and archived.

The post-mission data processing branches to two highly interactive parallel paths and both are still ongoing as of this writing. One path is to generate the precision position and attitude data records (PADR) for the entire mission[3]. The data source is the telemetry acquired during the mission, mainly the AODA sensor measurements. The other path is to fine tune the image and topography processors by using the actual high rate data collected by C-RADAR during the mission[4]. These two paths are highly interactive because the precision PADR file is needed for topographic construction. Here we briefly describe the intermediate products leading to the PADR.

From the complete mission telemetry, two products were generated. The first one is the system temperature file, which contains the history of the temperature sensors strategically placed on payload structure and inside the electronics. Calibration was applied to each temperature sensor to ensure accuracy of the measurements. The temperature file serves as input a finite-element structure thermal model to generate structure deformation records induced by thermal variation during the mission. The structure deformation records contain structural deviation from pre-mission model of several critical locations that could affect the metrology accuracy. The second file is the shuttle thruster firing records, which contain the time history of when the orbiter fired its Vernier thrusters. The structure deformation records and the thruster firing records are incorporated in the AODA data processing to correct for their respective effects. The primary data source for AODA processing is the measurements acquired by the AODA sensor suite. Some sensor data has to go through additional processing, e.g. the GPS measurements, to achieve the best attainable accuracy. The respective sensor data has to be assimilated, correcting for different time latencies between these measurements. And additional corrections, such as structure deformation, have to be included. Also the AODA data has to be time-synchronized with the C-RADAR data and the orbiter provided telemetry, which also has its latency. It turned out that quantifying these latencies and correcting for them were not trivial and often an incorrect adjustment would manifest in the excessive topographic fluctuation or discontinuities of the otherwise flat ocean data. The two data processing paths – generation of PADR and fine-tuning the topographic processor – became interactive and complementary to each other in verifying the respective processors. While it is still two years away for the near-global DEM will be finally produced, the post-flight processing activities so far indicate that the DEM will meet the required specifications.

6. CONCLUSION

As the first fixed baseline InSAR dedicated to collecting data for the generation of near-global DEM, SRTM flight is a resounding success. This paper can only highlight some of the interesting and challenging aspects of the C-band InSAR implementation, and the considerations went into the implementation. The systems engineering process in establishing system architecture, allocating the requirements, defining the interfaces, verifying the design, and operating the instrument was challenging, not only for the complexity of the system but also in the tightly couple nature of each element in the design. To enable topography generation, each system needs to perform to its specifications but each system's specifications are contingent on other systems meeting their specifications. For example, AODA specifications can only be met if AMS meets its specifications and some errors can be reallocated from one system to another as part of the trade. It is in these aspects that make the InSAR more challenging than the more conventional SAR. The considerations and the processes used for SRTM implementation are applicable to future spaceborne InSAR missions. For example, the automatic beam tracker, which was not used throughout the mission, would be required for a formation-flight InSAR systems. The past and ongoing SAR missions – SIR-C, ERS-1/2, RADARSAT and JERS-1 – have demonstrated wide applications of SAR and the advent of

InSAR significantly broaden the usefulness of SAR. We fully expect the trend to continue. Higher resolution SAR and InSAR, approaching that can be obtained by optical sensors, will be compelling for applications that require greater accuracy. SAR and InSAR with focused scientific objectives will also be flown to address the needs for selective and synergistic disciplines. For example, a wide-swath low-resolution dual-polarization SAR system could be flown for hydrology, free-thaw and biomass applications. Another example is a dedicated repeat-track InSAR system for change detection in surface deformation and glacier motion monitoring. Although SRTM flight duration is short, its significance lies not only that it would provide the first uniform near-global DEM with unprecedented resolution, but also that it has demonstrated the power of InSAR and that the implementation of such a system is within the reach of technology.

ACKNOWLEGEMENTS

A complicated and groundbreaking system such as SRTM could not be implemented without a highly competent and dedicated team. To fly such a payload on the Space Shuttle required all participating agencies to work as a close-knit team. The successful flight of SRTM is testimonial to such a tremendous team effort. The authors in particular wish to thank the core system engineering team members, who not only led the technical design and implementation of their respective subsystem but also contributed to the entire system engineering effort. The work reported herein was performed at the Jet Propulsion Laboratory (JPL), California Institute of Technology, under contract with U.S. National Aeronautics and Space Administration (NASA). The SRTM Project is jointly funded by NASA and U.S. National Imagery and Mapping Agency (NIMA) and the X-SAR portion is funded by the German Space Agency (DLR).

REFERENCES

1. P. A. Rosen, S. Hensley, I. R. Joughin, F. K. Li, S. N. Madsen, E. Rodriguez, and R. Goldstein, "Synthetic Aperture Radar Interferometry," *Proceedings of the IEEE,* vol. 88, no. 3, pp. 333-382, 2000.
2. D. L. Evans, J. J. Plaut, and E. R. Stofan, "Overview of the Spaceborne Imaging Radar-C/X-Band Synthetic Aperture Radar (SIR-C/X-SAR) Missions," *Remote Sensing Env.,* vol. 59, no. 2, pp. 135-140, 1997.
3. E. Wong, W. Breckenridge, D. Boussalis, P. Brugarolas, "Attitude determination for the Shuttle Radar Topography Mission," *AIAA-99-3968,* AIAA Guidance, Navigation, and Control Conference, Portland, Oregon, 1999.
4. S. Hensley, P. A. Rosen, "Topographic Map Generation from SRTM C-Band SCANSAR Interferometry," *Proceedings of SPIE,* vol. 4152, SPIE's Second International Asia-Pacific Symposium on Remote Sensing of the Atmosphere, Environment, and Space (this conference), Sendai, Japan, 2000.